Modelling of locomotion systems using deformable magnetizable media

2006 J. Phys.: Condens. Matter 18 S2973

(http://iopscience.iop.org/0953-8984/18/38/S30)

INSTITUTE OF PHYSICS PUBLISHING JOURNAL OF PHYSICS: CONDENSED MATTER

J. Phys.: Condens. Matter **18** (2006) S2973–S2983 doi:10.1088/0953-8984/18/38/S30

Modelling of locomotion systems using deformable magnetizable media

K Zimmermann[1], V A Naletova[2], I Zeidis[1], V Böhm[1] and E Kolev[1]

[1] Faculty of Mechanical Engineering, Technische Universitaet Ilmenau, PF 100565, 98684, Ilmenau, Germany
[2] Department of Mechanics and Mathematics, MV Lomonosov Moscow State University, 119992, Moscow, Russia

E-mail: klaus.zimmermann@tu-ilmenau.de and naletova@imec.msu.ru

Received 16 May 2006, in final form 10 July 2006
Published 8 September 2006
Online at stacks.iop.org/JPhysCM/18/S2973

Abstract

This paper deals with the modelling and the realization of active and passive locomotion systems using the effects of the deformation of a magnetizable elastic material and the deformation of the surface of a membrane filled with a ferrofluid under the influence of a magnetic field. Prototypes implementing these principles have been constructed and proved positive. Theoretically (analytically and numerically) calculated results of the velocity of the mobile system are compared with the experimental data. Artificial worms based on these principles could be autonomous systems, and could be useful in medicine and in inspection technology.

(Some figures in this article are in colour only in the electronic version)

1. Introduction

On observing the locomotion of worms, one recognizes a conversion of (mostly periodic) internal deformations into a change of external position (undulatory locomotion). The realization of a motion using the deformation of magnetizable materials (a magnetic fluid or a magnetizable polymer) in a magnetic field is an actual problem. The deformation of a surface of a magnetic fluid in a travelling magnetic field is used in pumps with magnetic fluids. In Zimmermann *et al* (2004a, 2004b) the theory of a flow of layers of magnetizable fluids in a travelling magnetic field is considered. It is shown that the travelling magnetic field can create a flux in the fluid layers. This effect can be applied for the realization of locomotion.

Compact locomotion devices using the deformation of magnetizable materials in the applied magnetic field (Turkov 2002) are a new interesting problem. The initiator of motion in such a device is an alternate magnetic field, which conforms to exterior sources (electromagnetic system or motion permanent magnets). A micro-robot with individual cells corresponding to the earthworm's segment and sealed with water-based magnetic fluid has been

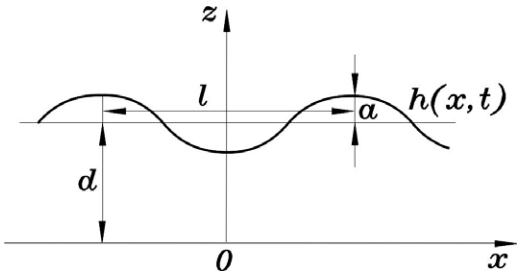

Figure 1. Magnetic fluid layer.

developed by Saga and Nakamura (2002, 2004). In Zimmermann *et al* (2004c), the theoretical study of the behaviour of a locomotion system using periodic deformation of a magnetizable polymer is done, when an alternate uniform magnetic field operates. The average velocity of such locomotion systems is proportional to the difference of the friction coefficients between the system and the substrate, which depends on the directions of motion.

Worm-like locomotion systems show their advantages in inspection techniques and medical applications (endoscopy). These areas of application were considered by Choi *et al* (2002), Mangan *et al* (2002), Menciassi and Dario (2003). In Choi *et al* (2002) an actuator based on a dielectric elastomer is used. In the present paper theoretical and experimental possibilities of using deformable magnetizable media as actuators for mobile medical robots are investigated.

The undulatory locomotion of an artificial worm is based on travelling waves on its surface. Therefore the expression for the magnetic field strength creating a sinusoidal wave on the surface of a viscous magnetic fluid as a function of the characteristics of the fluid (viscosity, surface tension, and magnetic permeability) and the parameters of the wave are obtained in the first theoretically oriented part of the paper.

In the second part of the present paper the motions of three samples of a magnetizable body (magnetizable worm) in an alternate magnetic field are studied experimentally for a large diapason of the electromagnetic system frequency. The prolate bodies of the magnetizable composites (an elastic polymer and solid magnetizable particles) and a capsule with a magnetic fluid are used. The analytical estimation and numerical calculation of the deformation of the bodies in applied magnetic field and of the velocity of the bodies are done.

A deformable magnetizable worm in a magnetic field is a prototype of a mobile crawling robot. Such devices have some characteristics, which allow us to use them in medicine and biology. For example, they do not contain solid material contacting with a surrounding medium and they moves autonomously.

The third part of the paper deals with fundamental investigations necessary for the design and the application of segmented artificial worms, which have the earthworm as living prototype, and of new passive locomotion systems. The most important question in this interconnection is the estimation of the pressure distribution in the magnetic fluid under the influence of a controlled magnetic field.

2. Locomotion using a magnetic fluid in a travelling magnetic field

We consider a plane flow of an incompressible viscous magnetic fluid layer along a horizontal surface in a nonuniform magnetic field (see figure 1). The magnetic permeability of the fluid μ is assumed to be constant. The pressure on the free fluid surface is constant. In the case

of a constant magnetic permeability, the body magnetic force is absent and the magnetic field manifests itself in a surface force acting on the free surface (Rosensweig 1985).

Gravity is not taken into account. In this case, the system of equations consists of the continuity and Navier–Stokes equations:

$$\operatorname{div} \boldsymbol{V} = 0, \qquad \frac{\partial \boldsymbol{V}}{\partial t} + (\boldsymbol{V} \cdot \nabla)\boldsymbol{V} = -\frac{1}{\rho} \cdot \operatorname{grad} p + \frac{\eta}{\rho} \cdot \Delta \boldsymbol{V}. \tag{1}$$

Here, $\boldsymbol{V}$ is the velocity vector (u and w are the horizontal and vertical coordinates), p is the fluid pressure, η is the dynamic fluid viscosity coefficient, ρ is the fluid density, and t is time.

On the rigid substrate $z = 0$, the no-slip condition is satisfied:

$$\boldsymbol{V}(z = 0) = \boldsymbol{0}. \tag{2}$$

On the free surface $z = h(x, t)$, conditions of two types, kinematic and dynamic, should be satisfied. The kinematic condition is of the form

$$\frac{\mathrm{d}h}{\mathrm{d}t} = \frac{\partial h}{\partial t} + u\frac{\partial h}{\partial x} = w. \tag{3}$$

The dynamic conditions of continuity of the normal and tangential stresses on the free surface $z = h(x, t)$ take the form (neglecting the influence of the environment)

$$\left[-p + \gamma\frac{1}{R} + \frac{B_n^2}{8\pi}\left(\frac{1}{\mu} - 1\right) - \frac{H_t^2}{8\pi}(\mu - 1)\right]\boldsymbol{n} + \tau_{ij}n^j\boldsymbol{e}^i = \boldsymbol{0}. \tag{4}$$

Here, τ_{ij} are the viscous stress tensor components, R is the radius of curvature of the surface $z = h(x, t)$, $\boldsymbol{n}$ is the vector of outward normal to the surface, $\boldsymbol{e}^j$ are the basis vectors, γ is the film surface tension coefficient, and $B_n = \mu H_n$ is the normal component of the magnetic field strength vector. The magnetic field $\boldsymbol{H}$ is assumed to be fixed, since the non-inductive approximation implies $\mu - 1 \ll 1$. We will assume that the magnetic field creates the periodic travelling wave on the surface of a sufficiently thin layer (we denote the dimensional variables with the asterisk $*$):

$$h^*(x, t) = d + a\cos\left(\omega t^* - kx^*\right), \qquad \varepsilon = d \cdot k \ll 1.$$

We introduce the dimensionless variables

$$x = x^* \cdot k, \qquad z = z^*/d, \qquad h = h^*/d, \qquad \delta = a/d, \qquad u = u^*/U_c,$$
$$w = w^*U_c/\varepsilon, \qquad U_c = \omega/k, \qquad t = t^* \cdot \omega, \qquad p = p^*/P, \qquad P = \eta\omega/\varepsilon^2,$$
$$H^2 = H^{*2}/P, \qquad Re = \rho U_c d/\eta, \qquad W = \gamma d k^2/P.$$

For $\varepsilon \ll 1$, we will seek for a solution in the form of a power series in ε ($A \equiv h, u, w, p$):

$$A(x, z, t) = A_0(x, z, t) + \varepsilon \cdot A_1(x, z, t) + \cdots.$$

In the zeroth approximation in ε, for $Re < 1$ and $W = \mathrm{O}(1)$, using equations (1) and the conditions (2)–(4), we obtain an expression for the velocity components (subscript '0' is omitted):

$$u(x, z, t) = F(x, t)\left(\frac{z^2}{2} - hz\right), \qquad w(x, z, t) = F(x, t)\frac{\partial h}{\partial x} \cdot \frac{z^2}{2} + \frac{\partial F}{\partial x}\left(\frac{h}{2} \cdot \frac{z^2}{2} - \frac{z^3}{6}\right), \tag{5}$$

where $F(x, t) = \frac{\partial p}{\partial x}$.

The mass conservation law (1), condition (3), expression (5), and the assumption that $h(x, t) = h(\xi), \xi = t - x$ imply the following equation for the flow rate Q:

$$\frac{\partial h}{\partial t} + \frac{\partial Q}{\partial x} = 0, \qquad Q(x, t) = -Fh^3/3 = h + C. \tag{6}$$

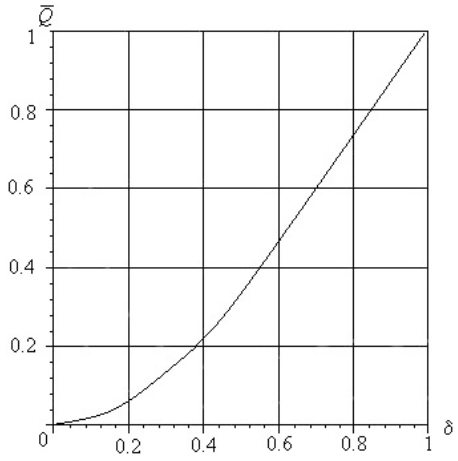

Figure 2. Average volume flow rate $\bar{Q}$ versus surface oscillation amplitude δ.

If the flow is T-periodic, we can introduce the average flow rate: $\bar{Q}(x) = \frac{1}{T}\int_0^T Q(x,t)\,\mathrm{d}t$. For $h(\xi) = 1 + \delta\cos(\xi)$, the dimensionless average flow rate is $\bar{Q} = 1 + C$.

Relation (4), with respect to (6), implies

$$W\frac{\partial^3 h}{\partial \xi^3} + \frac{(\mu-1)}{8\pi}\frac{\partial H^2}{\partial \xi} = -\frac{3}{h^2} - \frac{3C}{h^2}. \tag{7}$$

Using equation (7) it is possible to find the magnetic field creating the prescribed film shape:

$$H^2 = H_0^2 + \frac{8\pi}{\mu-1}\left(-W\frac{\partial^2 h}{\partial \xi^2} - 3\int\frac{1}{h^2}\,\mathrm{d}\xi - 3C\int\frac{1}{h^3}\,\mathrm{d}\xi\right), \qquad h(\xi) = 1 + \delta\cos(\xi), \quad \delta < 1. \tag{8}$$

The requirement for the magnetic field magnitude to change periodically leads to the expression $C = -2(1-\delta^2)/(2+\delta^2)$. The dependence of the average volume flow rate $\bar{Q} = 1 + C$ on the surface oscillation amplitude δ is shown in figure 2. The expression for the magnetic field (8) takes the form

$$H^2 = H_0^2 - D, \qquad D = \frac{8\pi}{\mu-1}\left(-W\delta\cos(\xi) + \frac{3\delta\sin(\xi)\,(2+\delta\cos(\xi))}{\left(2+\delta^2\right)(1+\delta\cos(\xi))^2}\right).$$

The constant H_0^2 can be chosen arbitrarily. However, this constant must not be less than the maximum value, $D_{\max} > 0$, of the function D in order not to violate the condition $H^2 \geqslant 0$. Thus we can assume $H_0^2 = D_{\max}$.

3. Magnetizable bodies in an alternate magnetic field

In the experiments we use cylindrically shaped bodies located in a cylindrical channel. The channel diameter d exceeds that (d_w) of the body. We denote the length of the body as l_w. The magnetic field is created by coils. The axes of the coils are in the horizontal plane, L is the distance between the axes of the coils and I is the current in the coils (see figure 3).

The coils are placed at the left- and right-hand sides of the channel. The magnetic field is created by three coils simultaneously (for example, coils numbers 6–8 in figure 3); the axis of the middle coil is the symmetry axis of the magnetic field.

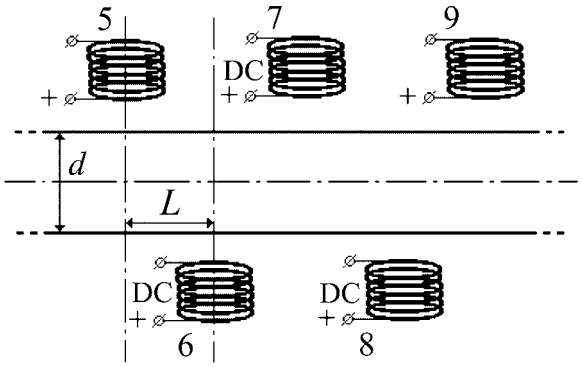

Figure 3. Arrangement of coils of the electromagnetic system.

Periodically, the left coil is switched off and the next coil is switched on; n is the number of coil switches per second (the frequency), so $T = 1/n$ is the period between change-over of the coils. The currents flowing through the coils are unidirectional. Such an electromagnetic system forms a travelling magnetic field $\boldsymbol{H}$, which is a complex function of x, y, z, t (x is the coordinate along the channel, z is parallel to axis of the coils, y is orthogonal to x and z).

It is shown experimentally that in such a periodic magnetic field the cylindrical magnetizable bodies move along the channel. The direction of the body motion is opposite to the direction of the travelling magnetic field.

3.1. The bodies from a magnetizable polymer

In the first experiment $I = 4.6$ A, $L = 10$ mm, $d = 11$ mm and the parameters of the 'worm' (sample 1) are as follows: Young's modulus $E_y = 50\,000$ Pa, length $l_w = 48$ mm, diameter $d_w = 4$ mm. The frequency n changes from 5 to 1000 s^{-1} in this experiment.

In the second experiment the parameters are $I = 4.6$ A, $L = 10$ mm, $d = 10$ mm, $l_w = 75$ mm, $d_w = 4.5$ mm, and sample 2 consists of a polymer with Young's modulus $E_y = 22\,000$ Pa. The frequency n changes from 5 to 1000 s^{-1}.

A cycle of body deformation by the travelling magnetic field is the process when the travelling magnetic field covers the body (see figure 4). At the end and beginning of this process the body is not deformed.

3.2. Elastic capsule filled with a magnetic fluid

In a third experiment an elastic cylindrical capsule filled with a magnetic fluid is inside a cylindrical channel. The channel and capsule diameters (d, d_c) are 10 and 4 mm. The length of the capsule filled with magnetic fluid l_c is 75 mm.

In our experiments the frequency n changes from 5 to 1000 s^{-1}. The phases of deformation of the capsule are shown in figure 5. The direction of the worm motion is opposite to the direction of the travelling magnetic field.

4. Comparison of theoretical and experimental results with respect to the body velocity

The body velocity depends on the geometrical shape of the deformed body and that of the channel. If n is small enough and the body inertia does not affect the body velocity, the

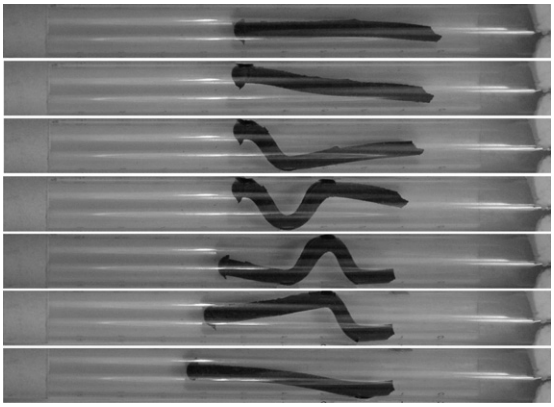

Figure 4. Magnetizable elastic body (sample 1) in the travelling magnetic field.

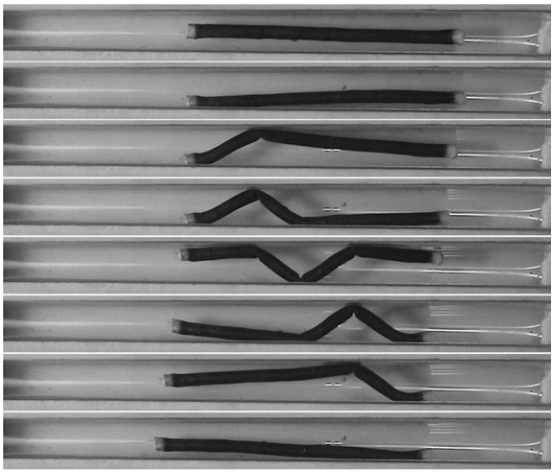

Figure 5. The form of the capsule at different moments in the travelling magnetic field.

following formula is valid:

$$v = k_s\,(l_s - L)/t_c, \qquad t_c = (k_s + 3)\,T, \qquad k_s = \left[l_w/l_s\right]. \tag{9}$$

Here l_s is the segment length (a segment is a part of deformed body between two neighbouring coils), k_s is the number of the segments, the symbol $[\cdots]$ denotes the integral part of the number, and t_c is the time of a cycle. The length of the segment may be determined under an assumption about its form. A segment form is determined by the elastic and magnetic properties of the body material, and the value of the magnetic field.

The problem of determination of the body form is very complex and here we consider three assumptions about the segment form.

4.1. Sinusoidal form

Let us assume that the segment of the body between two coils has sinusoidal form. In this case the equation of the central line of the segment is as follows:

$$y_S = 0.5\,(d - d_w)\sin(\pi x/L)\,.$$

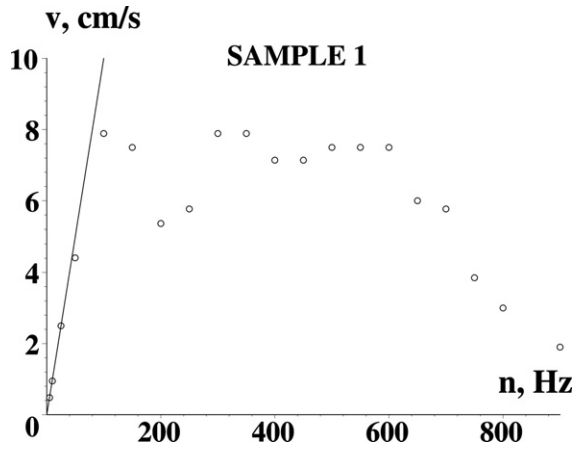

Figure 6. Body velocity $v = v(n)$ (sample 1).

For parameters $L = 10$ mm, $d = 11$ mm, $l_w = 48$ mm, $d_w = 4$ mm, the length of the sinusoidal segment is $l_s = 12.6$ mm, $k_s = 4$. The analytical estimation of the body velocity is determined as $v = 1.46n$ mm s^{-1}.

4.2. Body form is determined by the model of elastic beam

Let us assume that the form of the segment of the body between two coils is determined by the model of the elastic beam without extension (the bending moment is due to the magnetic forces, assuming that magnetic forces act on the ends of the segment). In this case the equation of the central line of the segment is as follows:

$$y_E = ax^3 + bx^2 + d_w/2,$$

where $a = -2\,(d - d_w)/L^3$, $b = 3\,(d - d_w)/L^2$.

For this assumption and for parameters as above the length of the segment is equal to 12.5 mm, $k_s = 4$ and the analytical estimation of the body velocity is $v = 1.43n$ mm s^{-1}.

4.3. Body form is a broken line

Let us assume that the form of the body segment between two coils is a straight line. The equation of the central line of the segment is as follows:

$$y_R = (d - d_w)\,x/L.$$

In this case for parameters as above the length of the segment is 12.2 mm, $k_s = 4$ and the analytical estimation of the body velocity is $v = 1.26n$ mm s^{-1}.

5. Discussion of results

From figure 6 we can see that for $n < 100$ s^{-1} the theoretical result (the body form is determined by the model of an elastic beam) matches with the experimental data for sample 1 for the first experiment. The maximal obtained body velocity is $v = 7.89$ cm s^{-1} for $n = 100$ s^{-1}. For $n > 950$ s^{-1} in the first experiment sample 1 does not move. The theoretical dependence of the body velocity on n and experimental data (sample 2) are shown in figure 7. Here for theoretical estimation we use the model of elastic beam and obtain that

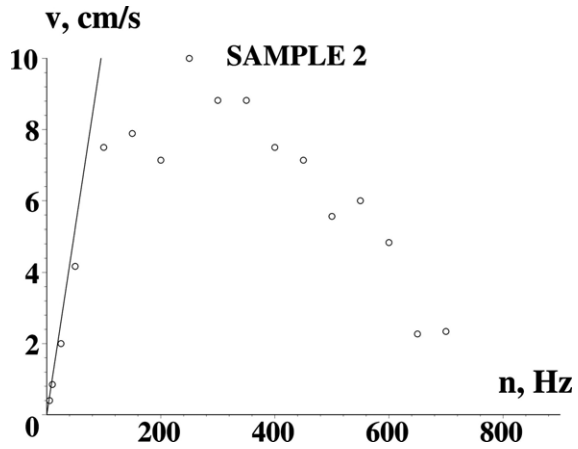

Figure 7. Body velocity $v = v(n)$ (sample 2).

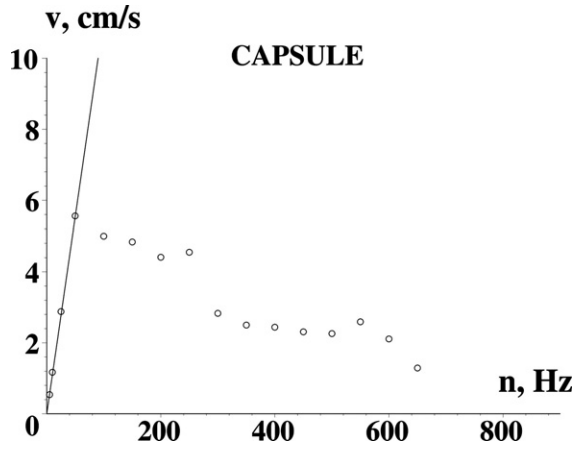

Figure 8. Body velocity $v = v(n)$ (a capsule with a magnetic fluid).

$v = 0.105n$ mm s^{-1}. From figure 7 we can see that for $n < 100$ s^{-1} the theoretical result matches with the experimental data for sample 2. The maximal obtained body velocity is 10 cm s^{-1} for $n = 250$ s^{-1}. For $n > 750$ s^{-1} sample 2 does not move.

From the third experiment it follows that the segment form of the capsule is a straight line. The length of the segment is determined by the formula

$$l_s = \sqrt{L^2 + (d - d_c)^2} = 11.66 \text{ mm}, \qquad k_s = 6.$$

From (1) we find the dependence of the velocity of the body on n: $v = 1.1n$ mm s^{-1}. The theoretical dependence of the velocity of the body v on n and experimental data are shown in figure 8.

For the frequency $n < 50$ s^{-1} the theoretical estimation of the velocity of the capsule matches with the experiments. In our experiment for $n > 700$ s^{-1} the capsule does not move.

The maximal obtained capsule velocity is $v = 5.56$ cm s^{-1} for $n = 50$ s^{-1}.

The body velocity depends on the geometrical shape of the deformed body and that of the channel. Only if n is small enough does the body inertia not affect the body velocity and formula (9) is valid.

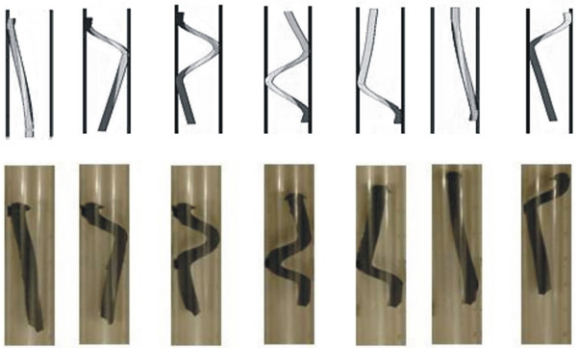

Figure 9. Analysis of the locomotion (sample 1) using the finite-element method for $n < 100\mathrm{Hz}$.

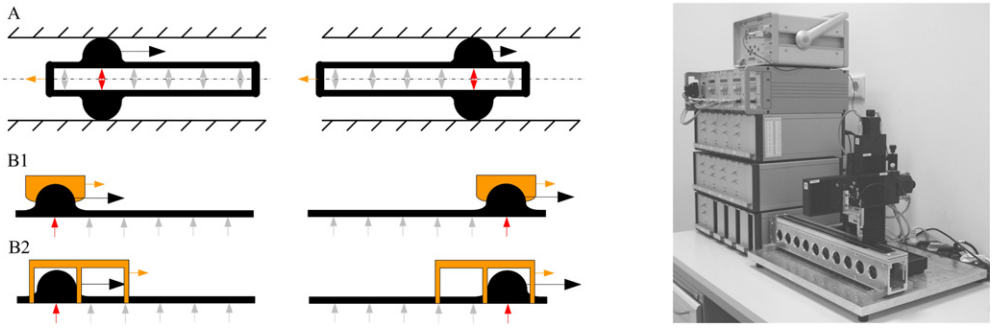

Figure 10. Schema of possible locomotion systems (left), and the experimental setup (right).

A simulation of the dynamic behaviour of the elastic body (sample 1) was made by the finite-element method (see figure 9). For $n < 100$ Hz the numerical results coincide with experimental data.

6. Design of active and passive locomotion systems and the interaction between a controlled magnetic field and a magnetic fluid

A moving magnetic field can generate a travelling wave on the surface of magnetic fluids. This travelling wave can be useful as a drive for locomotion systems. Therefore, peristaltically moving active locomotion systems could be realized with an integrated electromagnetic drive (see figure 10, left (A)). Also passive locomotion systems can be taken into account. Objects, which are on the surface of the fluid or are lying in the fluid, could be carried floating and/or shifting (see figure 10, left (B) and figure 13).

The following properties are important for the locomotion: (i) mass and geometry of the moving or moved object, (ii) the change of the shape and the position of the magnetic fluid, and (iii) the pressure distribution of the magnetic fluid with respect to the action of the moving magnetic field.

To analyse the behaviour of the magnetic fluids (under the described action of the magnetic field) and such locomotion systems, the experimental setup consists of 20 consecutively arranged cascaded electromagnets (one coil generates 3000 A turns). The measurement system

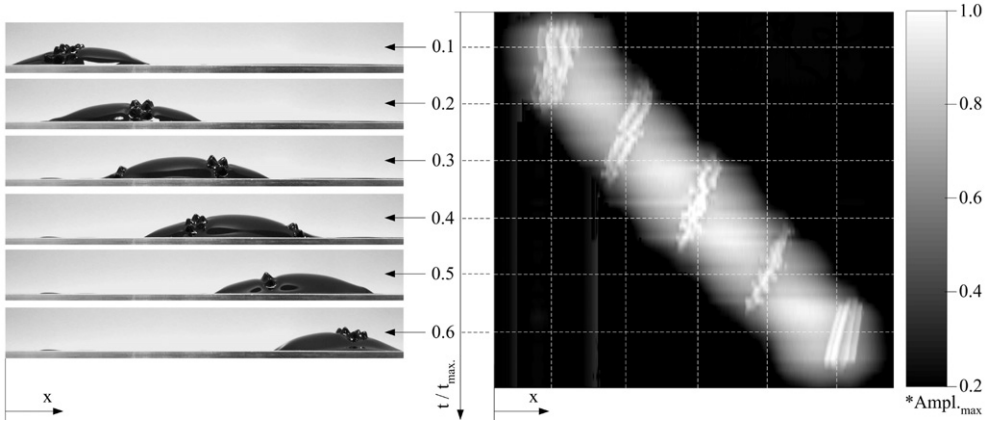

Figure 11. Travelling wave generated by a moving magnetic field.

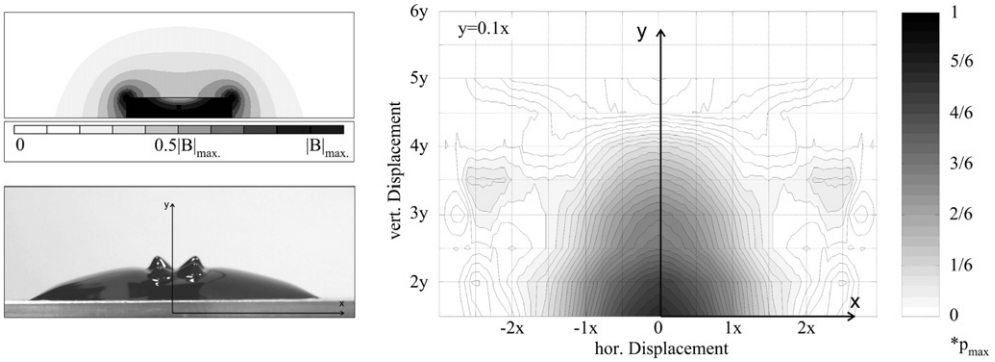

Figure 12. Schematic presentation of the electric induction density of an excited coil (left top), the emerged shape of the magnetic fluid surface (left bottom), and the pressure distribution of the magnetic fluid (right).

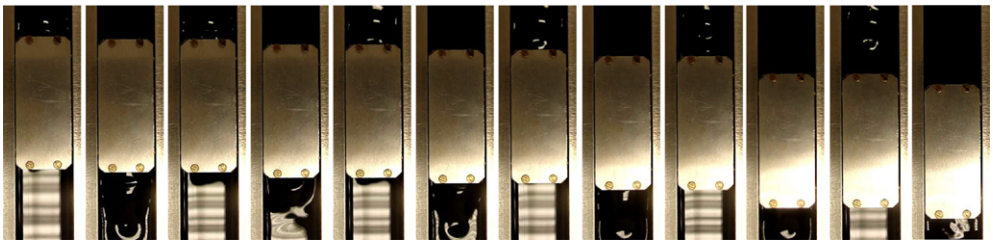

Figure 13. Example of passive locomotion by means of travelling waves in a magnetic fluid.

to detect the pressure of the fluid and the optical system to analyse the shape of the fluid are connected to a three-axis positioning unit (see figure 10, right). Figure 11 shows a travelling wave in a magnetic fluid.

Figure 12 shows schematically the magnetic field, which emerges from an electromagnet, the shape of the fluid and the pressure distribution.

In the experimental setup using a water-based ferrofluid a maximal change of the fluid pressure of about 2200 MPa was measured in the origin (see figure 12, right) after applying the magnetic field. Thus, it could be a realistic scenario to construct a cascaded structure of

cylindrical membranes filled with a magnetic fluid ('worm') and to get the necessary interaction between the 'worm' and the environment for peristaltic locomotion.

7. Conclusions

The expression for the magnetic field strength creating a sinusoidal wave on the surface of a viscous magnetic fluid as a function of the characteristics of the fluid (viscosity, surface tension, and magnetic permeability) and the parameters of the wave are obtained.

It is experimentally shown that in a specially structured periodic travelling magnetic field a cylindrical magnetizable elastic body moves along the channel. The direction of the body motion is opposite to the direction of the travelling magnetic field.

The maximal obtained body velocity is $v = 10$ cm s^{-1} for $n = 250$ s^{-1} (sample 2).

For the frequency $n < 100$ s^{-1} (samples 1 and 2) and for $n < 50$ s^{-1} (the capsule with the magnetic fluid) the theoretical (analytical and numerical) estimations of the velocity of the elastic body (the capsule with the magnetic fluid) coincide with the experimental data.

The creation of active biologically inspired locomotion systems and a new principle for a passive motion are possible using magnetizable media in controlled magnetic fields.

Acknowledgments

This work is supported by Deutsche Forschungsgemeinschaft (DFG, Zi 540/7-1) and the Russian Foundation for Basic Research (project 05-01-04001) and Grant Sci.Sc. 4474.2006.1.

References

Choi H R, Ryew S M, Jung K M, Kim H M, Jeon J W, Nam J D, Maeda R and Tanie K 2002 Microrobot actuated by soft actuators based on dielectric elastomer *Proc. IEEE/RSJ Int. Conf. Intell. Robots Syst.* **2** 1730–5

Mangan E V, Kingsley D A, Quinn R D and Chiel H J 2002 Development of a peristaltic endoscopie *Proc. IEEE Int. Conf. Robotics Automation* **1** 347–52

Menciassi A and Dario P 2003 Bio-inspired solutions for locomotion in the gastrointestinal tract: background and perspectives *Phil. Trans. R. Soc.* A **361** 2287–98

Rosensweig R E 1985 *Ferrohydrodynamics* (Cambridge: Cambridge University Press)

Saga N and Nakamura T 2002 Elucidation of propulsive force of micro-robot using magnetic fluid *J. Appl. Phys.* **91** 7003–5

Saga N and Nakamura T 2004 Development of a peristaltic crawling robot using magnetic fluid on the basis of locomotion mechanism of the earthworm *Smart Mater. Struct.* **13** 566–9

Turkov V A 2002 Deformation of an elastic composite involving a magnetic fluid *J. Magn. Magn. Mater.* **252** 156–8

Zimmermann K, Zeidis I, Naletova V A and Turkov V A 2004a Waves on the surface of a magnetic fluid layer in a travelling magnetic field *J. Magn. Magn. Mater.* **268** 227–31

Zimmermann K, Zeidis I, Naletova V A and Turkov V A 2004b Travelling waves on a free surface of a magnetic fluid layer *J. Magn. Magn. Mater.* **272–276** 2343–4

Zimmermann K, Zeidis I, Naletova V A and Turkov V A 2004c Modelling of worm-like motion systems with magneto-elastic elements *Phys. Status Solidi* **1** 3706–9